Carbohydrate Polymers 89 (2012) 111–116

Contents lists available at SciVerse ScienceDirect

Carbohydrate Polymers

journal homepage: www.elsevier.com/locate/carbpol

Characterization and antibacterial properties of genipin-crosslinked chitosan/poly(ethylene glycol)/ZnO/Ag nanocomposites

Yangshuo Liu, Hyung-Il Kim*

Department of Industrial Chemistry, Chungnam National University, Daejeon 305-764, Republic of Korea

ARTICLE INFO

Article history:
Received 4 November 2011
Received in revised form 21 February 2012
Accepted 21 February 2012
Available online 3 March 2012

Keywords:
Chitosan
Poly(ethylene glycol)
Zinc oxide
Silver
Antibacterial activity

ABSTRACT

Novel nanocomposites consisting of genipin-crosslinked chitosan (GC), poly(ethylene glycol) (PEG), zinc oxide (ZnO), and silver (Ag) nanoparticles were prepared for biomedical applications as the wound-healing materials. Various amounts of ZnO and Ag nanoparticles were dispersed in the GC/PEG hydrogel matrix without severe aggregation. The effects of composition and ZnO nanoparticles on the physico-chemical properties of nanocomposite samples were evaluated by infrared analysis, X-ray diffraction, and scanning electron microscopy. GC/PEG/ZnO/Ag nanocomposite showed the pH-sensitive swelling behavior and the improved mechanical properties. The antibacterial activities of nanocomposite films were tested toward the bacterial species *Escherichia coli*, *Pseudomonas aeruginosa*, *Staphylococcus aureus*, and *Bacillus subtilis*. GC/PEG/ZnO/Ag composite films had higher antibacterial activities than GC/PEG and GC/PEG/ZnO nanocomposite films. GC/PEG/ZnO/Ag composite films have potential application as wound and burn dressings.

1. Introduction

Dressing materials may inhibit bleeding, protect the wound from environmental irritants as well as water and electrolyte disturbances, and prevent invasion of microorganisms. Even though antibiotics have been greatly improved to deal with the increasing drug resistance of pathogens, it is also necessary to find advanced dressing materials which increase the drug resistance of pathogens effectively (Nagarajan & Rajagopalan, 2008; Seil & Webster, 2010; Zvekić, Srdić, Karaman, & Matavulj, 2011).

Zinc oxide (ZnO) has attracted wide interest because of its good photocatalytic activity, high stability, antibacterial property, and non-toxicity (Cohen, 2000; Sharma, Rao, Mathur, & Ameta, 1995; Wang, 2004). It was also reported that ZnO was found not to be cytotoxic to cultured human dermal fibroblasts (Zaveri et al., 2009). ZnO nanostructures have many important applications in biomedical fields (Riggio, Raffa, & Cuschieri, 2010), piezoelectric biosensors, food additives, and catalysis (Behnajady, Modirshahla, & Hamzavi, 2006; Brunner et al., 2006; Lu et al., 2011). Previous studies have demonstrated that ZnO exhibited antimicrobial activities on a broad spectrum of bacteria (Huang et al., 2008; Jones, Ray, Ranjit, & Manna, 2008; Li, Chen, & Jiang, 2007; Li et al., 2008). ZnO nanoparticles exert biocidal effects on bacterial, fungal, and viral species (Adams, Lyon & Alvarez, 2006). ZnO nanoparticles have recently received considerable attention due to their antimicrobial capabilities (Shafei & Abou-Okeil, 2011; Tayel et al., 2011; Vicentini, Smania, & Laranjeira, 2010). For economical and efficient use of ZnO, ZnO nanoparticle composites have been developed and tested for antimicrobial purposes. Additionally, doped silver (Ag) reduced the ionization energy of acceptors in ZnO and thus enhanced the emission (Chen, Zou, Bian, Sandhu, & Gao, 2011). Therefore, Ag ions can enhance the antimicrobial activity of ZnO.

Due to its intriguing biological properties, chitosan has long been known and used in pharmaceutical and biomedical applications (Enescu & Olteanu, 2008; Muzzarelli, 2009). Because of its unusual bioactivity, the formulation of chitosan with drugs has dual therapeutic effects, which make chitosan a novel candidate for drug carriers and antimicrobial activity (Muzzarelli et al., 1990). However, chitosan is difficult to apply to tissue engineering and artificial scaffolds because the chitosan film is very rigid and needs the plasticization. Poly(ethylene glycol) (PEG) is frequently used in the production of polymer blends. PEG could improve the flexibility and ductility of polymer by blending with the rigid polymer. PEG has many attractive properties, such as a wide range of molecular weights, excellent solubility in an aqueous medium, low toxicity, biocompatibility, and chain flexibility. PEG is readily excreted from the body via kidneys and forms non-toxic metabolites. The incorporation of PEG was expected to improve the biocompatibility of blend film (Zhang, Li, Gong, Zhao, & Zhang, 2002).

Genipin is manufactured from geniposide, a glucoside, by using beta-glucosidase. On the other hand, genipin is isolated in large quantity by a microbiological process involving *Penicillium nigricans* that produces beta-glucosidase that in turn hydrolyzes the geniposide into the aglycone genipin. It has been used over the

* Corresponding author. Tel.: +82 42 8217683; fax: +82 42 8218999.
E-mail address: hikim@cnu.ac.kr (H.-I. Kim).

0144-8617/$ – see front matter © 2012 Elsevier Ltd. All rights reserved.
doi:10.1016/j.carbpol.2012.02.058

years in traditional Chinese medicine to treat symptoms of type 2 diabetes (Danbuo, 1984; Zhang et al., 2006).

Films made from pure chitosan are very rigid (Budtova et al., 2002). Chitosan/PEG blend films may provide additional functionality as well as the flexibility compared to the pure chitosan films. Chitosan improves the mechanical properties and decreases water solubility of the PEG films, while PEG contributes to the formation of more flexible films. Chitosan and PEG-based membranes were prepared using glucose-mediating process (Wang & Hon, 2005). Genipin can form stable crosslinked products with enzymatic degradation resistance that is comparable to that of glutaraldehyde-fixed tissue.

This study aims to investigate the feasibility of a novel nanocomposite of genipin-crosslinked chitosan (GC)/PEG film in which various amounts of ZnO nanoparticles were embedded for the wound-dressing applications. In this study, GC/PEG/ZnO/Ag nanocomposite films with high antibacterial activities were successfully prepared via sol-cast transformation. The antibacterial efficiency of ZnO nanoparticles in GC/PEG hydrogels was investigated in terms of the characteristics of GC/PEG/ZnO/Ag nanocomposites. The antibacterial efficiency of the nanocomposites against *Escherichia coli* was analyzed for judging the feasibility of their use as wound dressings.

2. Experimental

2.1. Materials

Genipin and chitosan (medium molecular weight, 200 < viscosity <800 cP, 1% in 1% acetic acid, Brookfield) were purchased from Sigma–Aldrich. ZnO and Ag nanoparticles (<100 nm, 99.5% trace metals basis) were obtained from Aldrich Chemicals. PEG (Mw 4000) was purchased from Sigma. Acetic acid was purchased from Samchun Pure Chemical.

2.2. Microorganisms

The antibacterial activity of GC/PEG/ZnO/Ag nanocomposites was tested against four strains. *Staphylococcus aureus* (ATCC 25923) and *Bacillus subtilis* (ATCC 6633) are the Gram-positive bacteria. *E. coli* (ATCC 29522) and *Pseudomonas aeruginosa* (ATCC 27853) are the Gram-negative bacteria.

2.3. Preparation of GC/PEG/ZnO/Ag nanocomposites

Aqueous chitosan solution of 0.2% (w/v) was prepared by dissolving chitosan powder in aqueous 1% (v/v) acetic acid solution. Chitosan/PEG/ZnO/Ag solutions were prepared by mixing chitosan solution and PEG with various amounts of ZnO and Ag nanoparticles. 0.4 wt% of genipin was dissolved in 3 ml of water and then was added to the chitosan/PEG/ZnO/Ag mixed solutions under stirring for 8 h at room temperature to obtain a uniformly distributed and viscous solution. Films were prepared by casting the GC/PEG/ZnO/Ag nanocomposites onto plastic dishes. They were dried at room temperature for 48 h, and then further vacuum dried to remove any residual solvent. All films were neutralized in a 0.1 M NaOH solution for about 10 min, washed thoroughly with distilled water, and dried again. GC/PEG/ZnO/Ag nanocomposite films were stored in a desiccator at room temperature for further experiments. The formulation of GC/PEG/ZnO/Ag nanocomposites is shown in Table 1.

Table 1
Feed compositions of GC/PEG/ZnO/Ag nanocomposite films.

Sample name	Chitosan (g)	PEG (g)	ZnO (g)	Ag (mg)
GC/PEG-1	0.4	0.1	0	0
GC/PEG-2	0.4	0.1	0.01	0
GC/PEG-3	0.4	0.1	0.02	0
GC/PEG-4	0.4	0.1	0.04	0
GC/PEG-5	0.4	0.1	0.01	1
GC/PEG-6	0.4	0.1	0.02	1
GC/PEG-7	0.4	0.1	0.04	1
GC/PEG-8	0.4	0.1	0	1

2.4. Characterization of GC/PEG/ZnO/Ag nanocomposites

Fourier transform infrared attenuated total reflectance (FTIR-ATR) spectra of chitosan, PEG, GC/PEG interpenetrating polymer network (IPN), GC/PEG/ZnO/Ag nanocomposite films were recorded at room temperature by FTIR spectroscopy (FTS 175 C, Bio-Rad, USA) in the range 4000–500 cm^{-1} at a resolution of 2 cm^{-1}. The morphology of GC/PEG/ZnO/Ag nanocomposite films was investigated by scanning electron microscopy (SEM, JEM-1010, Jeol, Japan). Small pieces of nanocomposite films were cut and immersed in distilled water for 8 h. The SEM samples were prepared by freeze-drying at −70 °C under vacuum for 2 days, followed by coating with gold. Identification and quantitative determination of the various crystalline phases were studied using X-ray diffraction (XRD, RINT2000, Rigaku, Japan). The scanning of diffraction angle 2θ was between 5° and 40°.

2.5. Swelling study

The swelling behavior of GC/PEG/ZnO/Ag nanocomposite films was investigated by swelling the samples in the buffers of various pHs at room temperature. The wet weights of swollen samples were measured after blotting with a filter paper to remove the surface water, followed by immediate weighing. The swelling ratio of sample was expressed by the following equation:

$$\text{Swelling ratio } (\%) = \frac{(W_t - W_0)}{W_0} \times 100$$

where W_t and W_0 are the weights of the samples in the swollen and dry states, respectively. Each swelling experiment was repeated three times and the average values were reported.

2.6. Mechanical properties of GC/PEG/ZnO/Ag nanocomposites

The tensile strength and the elongation were measured using a universal testing machine (Instron 4200, Instron, USA). GC/PEG/ZnO/Ag nanocomposite films were cut to a size of 30 mm × 7 mm × 0.5 mm. The extension rate was 10 mm/min. The tensile strength and the elongation at failure were obtained from the load extension curves.

2.7. Evaluation of antibacterial activities

In vitro antibacterial activities of GC/PEG/ZnO/Ag nanocomposite films against *E. coli* as the indicator bacteria were evaluated by adopting the cell-counting method. Nutrient broth (Difco) was used as a growing medium for the microorganism. *E. coli* was grown aerobically in the nutrient broth at 37 °C for 24 h. GC/PEG/ZnO/Ag nanocomposite films of 10 mm diameter were then added and the mixtures of GC/PEG/ZnO/Ag nanocomposite and *E. coli* were placed at 37 °C in a shaking incubator for 6 h. The diluted bacterial solution was then spread on an agar dish. The bacteria were cultured for another 24 h and counted using the counter. The agar plate is divided into 3 sections GC/PEG, GC/PEG/ZnO, and GC/PEG/ZnO/Ag sample. Then the antibacterial activities of the samples were evaluated by the diameter of the intact region in agar plate.

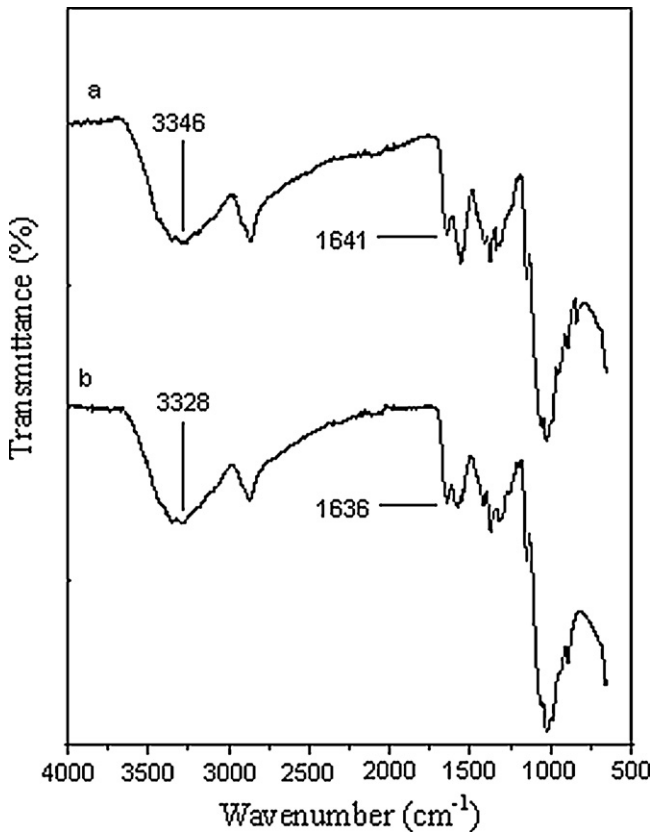

Fig. 1. FTIR spectra of (a) GC/PEG and (b) GC/PEG/ZnO/Ag (GC/PEG-6) films.

3. Results and discussion

3.1. FTIR spectroscopy

Fig. 1 shows the FTIR-ATR spectra of GC/PEG and GC/PEG/ZnO/Ag films. GC/PEG film has shown absorption peaks at 1641 cm^{-1}, 1583 cm^{-1}, and 1325 cm^{-1} relating to amide I, amide II of C=O stretching vibrations, and N—H bending vibrations, respectively. The bands due to N—H and O—H stretching vibrations overlapped in the absorption peak at 3346 cm^{-1}. The bands corresponding to OH/NH_2 groups have shifted to 3328 cm^{-1} and became broader and stronger for GC/PEG/ZnO/Ag nanocomposite film. The favorable intermolecular interactions between these groups and nanoparticles caused the variations in the characteristic absorption bands.

3.2. Surface morphology

Fig. 2 presents the SEM micrographs of the surfaces of GC/PEG, GC/PEG/ZnO, and GC/PEG/ZnO/Ag nanocomposite films. GC/PEG film showed the smooth surface morphology. ZnO and Ag nanoparticles were uniformly distributed on the surface of GC/PEG/ZnO and GC/PEG/ZnO/Ag nanocomposites without severe aggregation. GC/PEG/ZnO/Ag nanocomposite film has smooth surface texture and the spherical ZnO and Ag nanoparticles with diameters of about 25–65 nm were observed.

3.3. X-ray diffraction

Fig. 3 shows the XRD patterns of GC/PEG, GC/PEG/ZnO, and GC/PEG/ZnO/Ag nanocomposite films. Two crystal forms existed in GC/PEG film (Fig. 3a) depicting the major crystalline peaks at

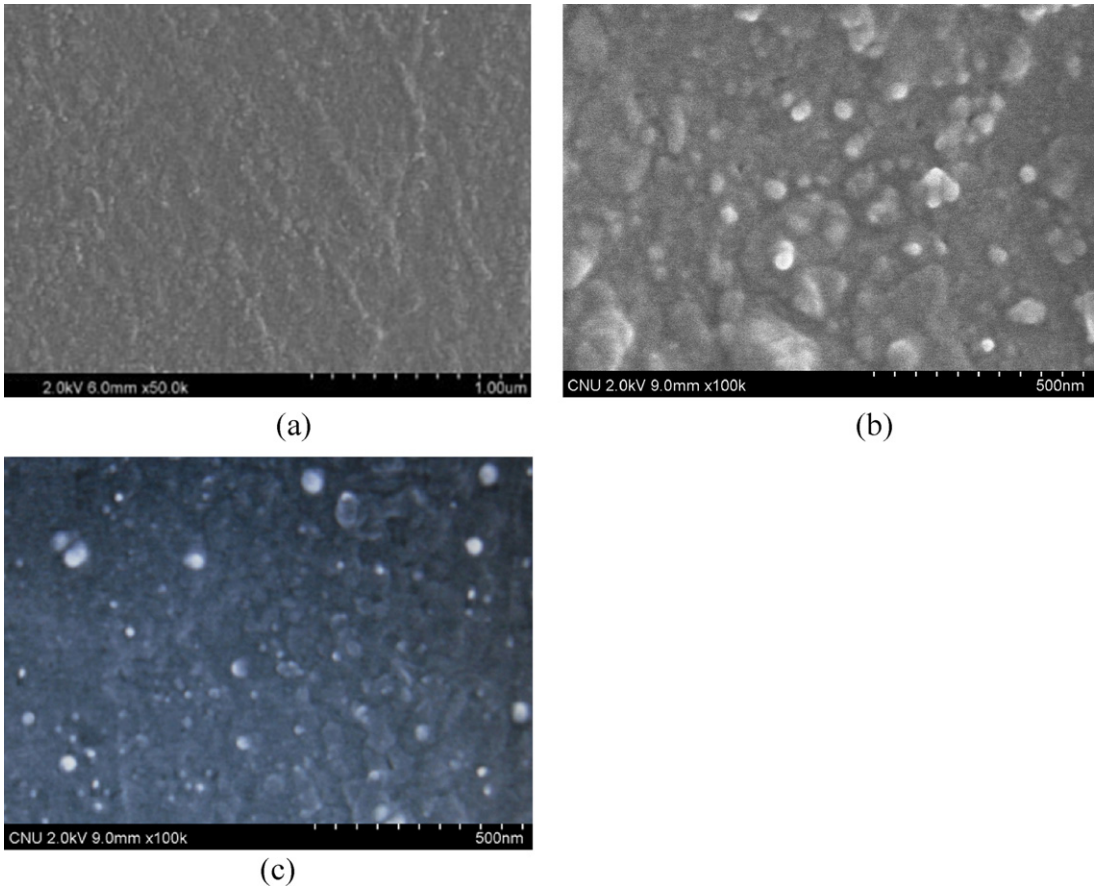

Fig. 2. SEM micrographs of (a) GC/PEG, (b) GC/PEG/ZnO (GC/PEG-3) and (c) GC/PEG/ZnO/Ag (GC/PEG-6) nanocomposites.

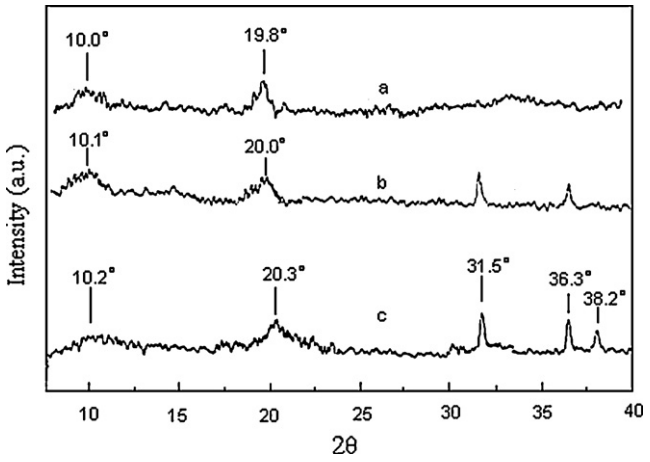

Fig. 3. X-ray diffraction patterns of (a) GC/PEG, (b) GC/PEG/ZnO (GC/PEG-3), and (c) GC/PEG/ZnO/Ag (GC/PEG-6) nanocomposite films.

10.0° and 19.8°, respectively. These two main XRD peaks of GC/PEG shifted to10.2° and 20.3° for GC/PEG/ZnO/Ag nanocomposite film (Fig. 3c). GC/PEG/ZnO/Ag nanocomposite film showed two additional peaks at 2θ of 31.5° and 36.3° which were related to the ZnO crystallite and another peak at 2θ of 38.2° which was characteristic of the Ag nanoparticles. These findings indicate the possible interactions between free hydroxyl groups of chitosan and ZnO and Ag nanoparticles in the nanocomposites.

3.4. Swelling behavior of GC/PEG/ZnO/Ag nanocomposites

The swelling behavior of GC/PEG, GC/PEG/ZnO, and GC/PEG/ZnO/Ag nanocomposites at various pHs is shown in Fig. 4. The swelling of GC/PEG matrix was pH-dependent. GC/PEG/ZnO/Ag nanocomposite swelled greatly in the acidic medium compared to the neutral or basic one. As ZnO and Ag nanoparticles were incorporated in GC/PEG matrix, the swelling decreased to some extent.

GC/PEG/ZnO/Ag nanocomposites swelled higher at a much faster rate in a lower pH medium than in a higher pH medium. The effect of pH on the swelling of the chitosan-containing hydrogels is ascribed to the hydrolysis of amide linkages in the crosslinked chitosan network by acid and the regeneration of amine groups in networks (Huang, Sung, Tsai, & Huang, 1998; Sung, Huang, Chang, Huang, & Hsu, 1999). Because the amino groups reformed in the

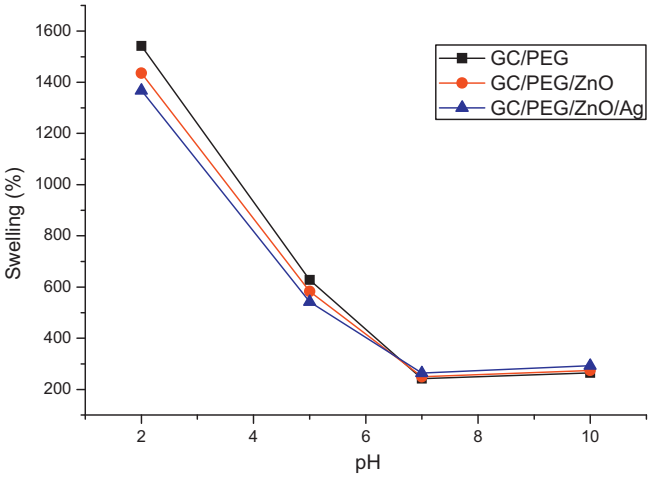

Fig. 4. Swelling ratios of GC/PEG, GC/PEG/ZnO (GC/PEG-3), and GC/PEG/ZnO/Ag (GC/PEG-6) nanocomposites at various pHs.

Table 2
Mechanical properties of GC/PEG, GC/PEG/ZnO, and GC/PEG/ZnO/Ag nanocomposite films.

Sample name	Tensile strength (MPa)	Elongation at break (%)
GC/PEG-1	56.7	16.2
GC/PEG-2	80.2	24.4
GC/PEG-3	70.4	14.3
GC/PEG-4	58.2	7.2
GC/PEG-5	85.5	25.5
GC/PEG-6	76.6	14.9
GC/PEG-7	62.1	7.4
GC/PEG-8	59.8	17.1

network could be protonated in acidic medium, the equilibrium swelling ratio of chitosan-containing hydrogel in the acidic solution was larger than that in the neutral one. The electrostatic repulsion of the protonated $-NH_3^+$ groups along the chitosan chain could lead to an expansion of the network and hence a higher swelling. Various hydrogel films were used in treating the chronic wounds such as burns and ulcers because good hydration was recognized to be important for quick healing and reepithelialization of the wound (Junichi, Norio, & Kensuke, 2008; Seabra & De Oliveira, 2004; Sen & Avc, 2005; Yu et al., 2007). However, a distinctive disadvantage of the commercially available wound dressing films is that they do not provide a barrier against wound infection, which limits their applicability.

3.5. Mechanical properties

Many synthetic and natural polymeric materials are developed to treat the burn wounds as antibacterial materials. However, they have limited applicability due to poor mechanical properties as well as lower rates of water absorption. ZnO and Ag-containing GC/PEG nanocomposites were developed in the present study to have better mechanical strength. The mechanical properties of GC/PEG, GC/PEG/ZnO, and GC/PEG/ZnO/Ag nanocomposite films are presented in Table 2. Both GC/PEG/ZnO and GC/PEG/ZnO/Ag nanocomposite films generally showed the higher tensile strength compared to GC/PEG film.

Among the various nanocomposite films, the nanocomposite films (GC/PEG-2 and GC/PEG-5) containing 0.01 g ZnO showed the highest mechanical properties. However, further increase in the ZnO content resulted in the fast deterioration of both tensile strength and elongation at break. Thus, the mechanical properties of GC/PEG film can be improved significantly by incorporating a proper amount of ZnO because of the favorable interactions between GC/PEG and ZnO nanoparticles. When ZnO was introduced in GC/PEG matrix, the intermolecular hydrogen bonds between GC and PEG were weakened and new hydrogen bonds were formed between GC and ZnO, which made the movement of macromolecular chain easier.

3.6. Antibacterial activity of GC/PEG/ZnO/Ag nanocomposites

ZnO nanoparticles embedded in GC/PEG matrix were responsible for the antibacterial activities. The antibacterial activities of GC/PEG, GC/PEG/ZnO, and GC/PEG/ZnO/Ag nanocomposite films were tested toward antibacterial activity against Gram-negative and Gram-positive bacteria by the inhibition zone method and presented in Table 3. It was found that GC/PEG without ZnO was able to inhibit the bacterial growth to some degree. However, the inhibition zone increased significantly when ZnO was incorporated and the content of ZnO increased. In addition, the antibacterial activity was improved more effectively by doping ZnO with small amount of Ag. The synergistic antibacterial activity of nanocomposites could be obtained by combining ZnO and Ag nanoparticles. Yoon, Byeon,

Table 3
Variation of diameters (mm) of the inhibition zone against bacteria.

Sample name	Gram-positive		Gram-negative	
	S. aureus	*B. subtilis*	*E. coli*	*P. aeruginosa*
GC/PEG-1	10.2	9.5	8.1	10.8
GC/PEG-2	11.9	10.4	10.1	12.4
GC/PEG-3	12.8	12.6	11.9	13.1
GC/PEG-4	16.5	15.6	15.1	15.4
GC/PEG-5	15.7	15.1	13.0	15.5
GC/PEG-6	18.1	17.4	17.2	18.6
GC/PEG-7	21.3	21.9	20.4	20.2
GC/PEG-8	11.1	11.4	9.2	11.0

Park, and Hwang (2007) observed that *B. subtilis* was more sensitive than *E. coli* to the nanoparticles, meaning that *E. coli* was more resistive to nanoparticles than *B. subtilis* was. They concluded that the lower sensitivities of *E. coli* as compared to *B. subtilis* was due to the outer membrane of Gram-negative bacteria such as *E. coli*, which was predominantly constructed from tightly packed lipopolysaccharide molecules resulting in the effective resistive barrier against nanoparticles. Fig. 5 shows the inhibition zone against *E. coli* formed on the culture plates after the antibacterial test. The smallest inhibition zone of 8.1 mm was obtained for GC/PEG film (Fig. 5a). However, the nanocomposite showed significantly improved inhibition effect on *E. coli* resulting in the inhibition zone of 11.9 mm for GC/PEG/ZnO (Fig. 5b) and 17.2 mm for GC/PEG/ZnO/Ag (Fig. 5c), respectively. GC/PEG films containing ZnO and Ag nanoparticles showed the highly improved antibacterial activity toward *E. coli*. GC/PEG/ZnO/Ag nanocomposite films prepared in this work may be used as hydrophilic wound and burn dressings (Vicentini et al., 2010).

3.7. Antibacterial mechanism

ZnO can produce electron–hole pairs under light irradiation of higher energy than its band gap energy (Liu, Morishima, Yatsui, Kawazoe, & Ohtsu, 2011). Electron–hole pairs (e^- h^+) are created to induce the redox reactions at the surface of ZnO. The hole (h^+) reacted with OH^- on the surface of ZnO nanoparticles, generating hydroxyl radicals ($OH^\bullet$), superoxide anion (O_2^-), and perhydroxyl radicals ($HO_2^\bullet$). These highly active free radicals damaged the cells of microorganism resulting in decomposition and complete destruction. The holes split H_2O molecules into OH^- and H^+. Dissolved oxygen molecules in aqueous medium are transformed to superoxide radical anions ($^\bullet O_2^-$), which in turn react with H^+ to generate ($HO_2^\bullet$) radicals, which produce hydrogen peroxide anions (HO_2^-) upon subsequent collision with electrons. Finally, various active oxygen species can oxidize the organic components of cell to carbon dioxide and water. Thus, ZnO can decompose common organic matters such as bacteria and viruses effectively.

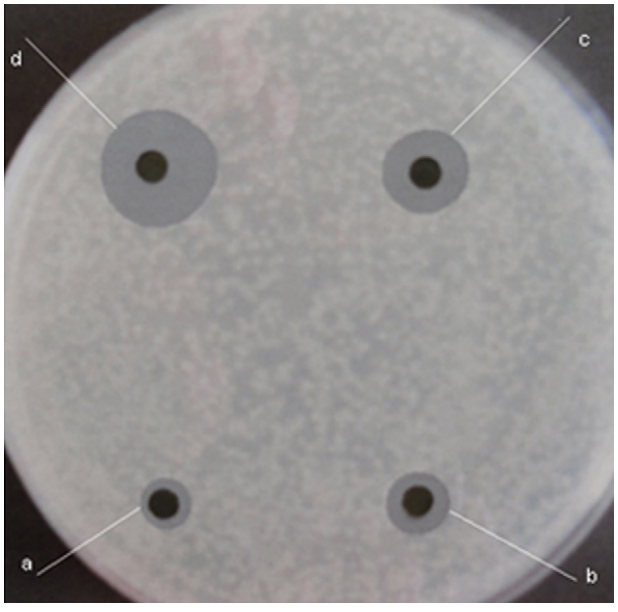

Fig. 5. Comparison of *E. coli* inhibition zones formed by (a) GC/PEG, (b) GC/PEG/Ag, (c) GC/PEG/ZnO (GC/PEG-3), and (d) GC/PEG/ZnO/Ag (GC/PEG-6) nanocomposite films.

The presence of transition metals such as Ag improved the charge transfer, reduced the chance of electron–hole pair recombination, and promoted the generations of perhydroxyl radicals and other strong oxidizing materials (Seki et al., 2010; Shchukin, Ustinovich, Sviridov, & Pichat, 2004). Therefore, the presence of Ag and ZnO enhanced the antimicrobial ability of chitosan significantly.

4. Conclusions

ZnO nanoparticles were uniformly distributed in GC/PEG matrix to form GC/PEG/ZnO nanocomposites. GC/PEG/ZnO nanocomposites showed the higher swelling ratios as the pH decreased to acidic condition. The presence of ZnO in GC/PEG matrix inhibited the proliferation of bacteria effectively. The antimicrobial activity of GC/PEG/ZnO nanocomposites increased as the content of ZnO increased. The antibacterial activity was improved more effectively by doping ZnO with small amount of Ag nanoparticles. GC/PEG/ZnO/Ag nanocomposites could be applied successfully as the antibacterial wound-dressing films based on both swelling and antibacterial characteristics.

References

Adams, L. K., Lyon, D. Y., & Alvarez, P. J. J. (2006). Comparative ecotoxicity of nanoscale TiO_2, SiO_2, and ZnO water suspensions. *Water Research*, *40*, 3527–3532.
Behnajady, M. A., Modirshahla, N., & Hamzavi, R. (2006). Kinetic study on photocatalytic degradation of C.I. acid yellow 23 by ZnO photocatalyst. *Journal of Hazardous Materials*, *133*, 226–232.
Brunner, T., Piusmanser, P., Spohn, P., Grass, R., Limbach, L., Ruinink, A. B., et al. (2006). In vitro cytotoxicity of oxide nanoparticles: comparison to asbestos, silica, and the effect of particle solubility. *Environmental Science and Technology*, *40*, 4374–4381.
Budtova, T., Belnikevich, N., Kalyuzhnaya, L., Alexeev, V., Bronnikov, S., Vesnebolotskaya, S., et al. (2002). Chitosan modified by poly(ethylene oxide): Film and mixture properties. *Journal of Applied Polymer Science*, *84*, 1114–1122.
Chen, R. Q., Zou, C. W., Bian, J. M., Sandhu, A., & Gao, W. (2011). Microstructure and optical properties of Ag-doped ZnO nanostructures prepared by a wet oxidation doping process. *Nanotechnology*, *22*, 105706–105713.
Cohen, M. L. (2000). The theory of real materials. *Annual Review of Materials Science*, *30*, 1–26.
Danbuo, Y. (1984). In Y. Wang (Ed.), *The essential methods for miscellaneous diseases*. PR China: People's Health Publishers.
Enescu, D., & Olteanu, C. E. (2008). Functionalized chitosan and its use in pharmaceutical, biomedical, and biotechnological research. *Chemical Engineering Communications*, *195*, 1269–1291.
Huang, L. L., Sung, H. W., Tsai, C. C., & Huang, D. M. (1998). Biocompatibility study of a biological tissue fixed with a naturally occurring crosslinking reagent. *Journal of Biomedical Materials Research*, *42*, 568–576.
Huang, Z., Zheng, X., Yan, D., Yin, G., Liao, X., Kang, Y., et al. (2008). Toxicological effect of ZnO nanoparticles based on bacteria. *Langmuir*, *24*, 4140–4144.
Jones, N., Ray, B., Ranjit, K. T., & Manna, A. C. (2008). Antibacterial activity of ZnO nanoparticle suspensions on a broad spectrum of microorganisms. *FEMS Microbiology Letters*, *279*, 71–76.
Junichi, T., Norio, M., & Kensuke, S. (2008). Characterization of chitosan/citrate and chitosan/acetate films and applications for wound healing. *Journal of Applied Polymer Science*, *110*, 608–615.
Li, Q., Chen, S. L., & Jiang, W. C. (2007). Durability of nano ZnO antibacterial cotton fabric to sweat. *Journal of Applied Polymer Science*, *103*, 412–416.
Li, Q. L., Mahendra, S., Lyon, D. Y., Brunet, L., Liga, M. V., Li, D., et al. (2008). Antimicrobial nanomaterials for water disinfection and microbial control: Potential applications and implications. *Water Research*, *42*, 4591–4602.
Liu, Y., Morishima, T., Yatsui, T., Kawazoe, T., & Ohtsu, M. (2011). Size control of sol–gel-synthesized ZnO quantum dots using photo-induced desorption. *Nanotechnology*, *22*, 215605 (5 pp).

Lu, X., Xu, Z., Yan, X. W., Li, S., Ren, W., & Cheng, Z. Y. (2011). Piezoelectric biosensor platform based on ZnO micro membrane. *Current Applied Physics*, *82*, 4806–4808.
Muzzarelli, R. A. A. (2009). Genipin crosslinked chitosan hydrogels as biomedical and pharmaceutical aids. *Carbohydrate Polymers*, *77*, 1–9.
Muzzarelli, R. A. A., Tarsi, R., Filippini, O., Giovanetti, E., Biagini, G., & Varaldo, P. E. (1990). Antimicrobial properties of N-carboxybutyl chitosan. *Antimicrobial Agents and Chemotherapy*, *34*, 2019–2023.
Nagarajan, P., & Rajagopalan, V. (2008). Enhanced bioactivity of ZnO nanoparticles—An antimicrobial study. *Science and Technology of Advanced Materials*, *9*, 035004, 7 pp.
Riggio, C., Raffa, V., & Cuschieri, A. (2010). Synthesis, characterisation and dispersion of zinc oxide nanorods for biomedical applications. *Micro & Nano Letters*, *5*, 355–360.
Seabra, A. B., & De Oliveira, M. G. (2004). Poly(vinyl alcohol) and poly(vinyl pyrrolidone) blended films for local nitric oxide release. *Biomaterials*, *25*, 3773–3782.
Seil, J. T., & Webster, T. J. (2010). Zinc oxide nanoparticle and polymer antimicrobial biomaterial composites. In *Bioengineering conference, proceedings of the 2010 IEEE 36th annual northeast* New York, NY, March 26–28, 2010, (2nd ed., pp. 1–2).
Seki, S., Sekizawa, T., Haga, K., Sato, T., Takeda, M., Seki, Y., et al. (2010). Effects of silver deposition on 405 nm light-driven zinc oxide photocatalyst. *Journal of Vacuum Science & Technology B*, *28*, 188–193.
Sen, M., & Avc, E. N. (2005). Radiation synthesis of poly (N-vinyl-2-pyrrolidone)-k-carrageenan hydrogels and their use in wound dressing applications. I. Preliminary laboratory tests. *Journal of Biomedical Materials Research Part A*, *74*, 187–196.
Shafei, A., & El Abou-Okeil, A. (2011). ZnO/carboxymethyl chitosan bionanocomposite to impart antibacterial and UV protection for cotton fabric. *Carbohydrate Polymers*, *83*, 920–925.
Sharma, A., Rao, P., Mathur, R. P., & Ameta, S. C. (1995). Photocatalytic reactions of xylidine ponceau on semiconducting zinc oxide powder. *Journal of Photochemistry and Photobiology*, *A86*, 197–200.
Shchukin, D., Ustinovich, E., Sviridov, D., & Pichat, P. (2004). Effect of silver deposits on the photocatalytic activity of titanium dioxide for the removal of 2-chlorophenol in water. *Photochemical and Photobiological Science*, *3*, 142–144.
Sung, H. W., Huang, D. M., Chang, W. H., Huang, R. N., & Hsu, J. C. (1999). Evaluation of gelatin hydrogel crosslinked with various crosslinking agents as bioadhesives: In vitro study. *Journal of Biomedical Materials Research Part A*, *46*, 520–530.
Tayel, A. A., El-Tras, W. F., Moussa, S., El-Baz, A. F., Mahrous, H., Salem, M. F., et al. (2011). Antibacterial action of zinc oxide nanoparticles against foodborne pathogens. *Journal of Food Safety*, *31*, 211–218.
Vicentini, D. S., Smania, A., Jr., & Laranjeira, M. C. M. (2010). Chitosan/poly (vinyl alcohol) films containing ZnO nanoparticles and plasticizers. *Materials Science and Engineering C*, *30*, 503–508.
Wang, J. W., & Hon, M. H. (2005). Preparation of poly(ethylene glycol)/chitosan membranes by a glucose-mediating process and in vitro drug release. *Journal of Applied Polymer Science*, *96*, 1083–1094.
Wang, Z. L. (2004). Zinc oxide nanostructures: Growth, properties and applications. *Journal of Physics: Condensed Matter*, *16*, R829–R858.
Yoon, K. Y., Byeon, J. H., Park, J. H., & Hwang, J. (2007). Susceptibility constants of *Escherichia coli* and *Bacillus subtilis* to silver and copper nanoparticles. *Science of the Total Environment*, *373*, 572–575.
Yu, H. J., Xu, X. Y., Chen, X. S., Lu, T. C., Zhang, P. B., & Jing, X. B. (2007). Preparation and antibacterial effects of PVA–PVP hydrogels containing silver nanoparticles. *Journal of Applied Polymer Science*, *103*, 125–133.
Zaveri, T., Dolgova, N., Chu, B. H., Lee, J., Lele, T., Ren, F., et al. (2009). Macrophage response to zinc oxide nanorod surfaces—Topography and toxicity. *25th southern biomedical engineering conference 2009. IFMBE proceedings* (pp. 119–120).
Zhang, M., Li, X. H., Gong, Y. D., Zhao, N. M., & Zhang, X. F. (2002). Properties and biocompatibility of chitosan films modified by blending with PEG. *Biomaterials*, *23*, 2641–2648.
Zhang, C. Y., Parton, L. E., Ye, C. P., Krauss, S., Shen, R., Lin, C. T., et al. (2006). Genipin inhibits UCP2-mediated proton leak and acutely reverses obesity- and high glucose-induced beta cell dysfunction in isolated pancreatic islets. *Cell Metabolism*, *3*, 417–427.
Zvekić, D., Srdić, V. V., Karaman, M. A., & Matavulj, M. N. (2011). Antimicrobial properties of ZnO nanoparticles incorporated in polyurethane varnish. *Processing and Application of Ceramics*, *5*, 41–45.